Pergamon

Cement and Concrete Research, Vol. 25, No. 6, pp. 1165-1178, 1995

0008-8846/95 $9.50+.00

0008-8846(95)00109-3

MICROSTRUCTURE, CRACK PROPAGATION, AND MECHANICAL PROPERTIES OF CEMENT PASTES CONTAINING HIGH VOLUMES OF FLY ASHES

M.H. Zhang
CANMET
Natural Resources Canada
405 Rochester Street
Ottawa, Canada K1A 0G1

(Refereed)
(Received July 1, 1994; in final form May 4, 1995)

ABSTRACT

This paper presents information on the effect of fly ashes on the microstructure of high volume fly ash (HVFA) pastes and how this affect the crack pattern and the stress-strain relationship. The HVFA pastes were prepared incorporating 58% of fly ashes. Fly ash particles appear to act as microaggregates in the pastes. Crack propagation generally deviates around the fly ash particles. Compared with that for the Portland cement paste of similar strength, the stress-strain curves for the HVFA pastes are less linear and begin to deviate at about 60-70% of the ultimate strength at 28 days. Based on these information, it was proposed that the HVFA paste may be considered as a composite material microscopically with fly ash particles as reactive microaggregates embedded in a matrix of hydration and reaction products. The effect of high volumes of fly ash on various properties of the concrete such as the modulus of elasticity, shrinkage and creep, as well as permeability were also discussed.

INTRODUCTION

Research has been conducted on the replacement of high volumes of Portland cement by fly ash in structural grade concrete at CANMET since 1985 [1,2,3,4]. Termed high-volume fly ash (HVFA) concretes, these materials are proportioned to contain more fly ash than Portland cement. From the perspective of their application for structural purposes, the most significant features of these concretes relate to their economy of production, mechanical properties, and durability.

Traditionally, fly ash content for structural concrete has been limited to about 20 to 25% of the cementitious materials. Codes and standards in many countries still set maximum limits of fly ash content for structural concrete. For concrete with 20 to 25% of fly ash, most of the fly ash

will generally react as a pozzolanic material. In the latest revision of the American Concrete Institute Building Code for Reinforced Concrete (ACI 318), fly ash and other pozzolans are recognized as a component of cementitous material when calculating water/cementioious materials ratio. In HVFA concrete, however, pozzolanic reaction of fly ash may not be complete because the fly ash content is relatively high in proportion to cement. A part of the fly ash may remain in the system even after a long time of curing. This may affect microstructure and various properties of HVFA paste, and consequently properties of HVFA concrete.

Previous investigations by CANMET have shown that HVFA concrete has excellent mechanical properties and durability [2,3]. The concrete has a higher modulus of elasticity, lower shrinkage and creep, and lower water permeability compared with those made with Portland cement of similar strength. Though considerable information is available on the engineering properties of HVFA concretes, basic properties of these materials are not well understood and many questions remain unanswered.

This paper presents information on the effect of fly ash on the microstructure of HVFA paste and how the microstructure affects the crack pattern and the stress-strain relationship. Based on this information, it was proposed that the HVFA paste may be considered as a composite material with fly ash particles as reactive microaggregates embedded in a matrix of hydration and reaction products. For information on the chemical factors of the HVFA system, reference is made to a paper by Berry et al. [5].

EXPERIMENTAL

An ASTM Type I cement and two types of fly ashes, a Class F ash from Georgia and a Class C ash from North Dakota were used in this study. Chemical composition and physical properties of the cement and the fly ashes are summarized in Table 1. The superplasticizer selected was a naphthalene based and was used as supplied by the manufacturer in the form of an aqueous solution containing 41.2 % solids by weight.

Pastes with a water to cementitious materials ratio of 0.3 and a 58 % mass replacement of portland cement by fly ash were prepared. The mix proportions and nomenclature used are given in Table 2. The pastes, designated GB and GL, were used for the examination of microstructure development; while those, designated E2 and E3, were used for the determination of mechanical properties and the examination of crack modes. A reduced quantity of superplasticizer was employed in Mixtures E2 and E3 in order to reduce bleeding in the larger specimens required for the testing of the mechanical properties.

After mixing, the paste samples for the examination of microstructure were sealed in plastic vials (about 25x40 mm) and cured at 21^{0}C. The paste samples for the examination of crack propagation were also cast in the plastic vials, but were cured in lime saturated water after demolding until the time of testing. For the determination of stress-strain relationships, specimens (50x150 mm cylinders) were prepared. Pastes from Mixtures E2 and E3 were demolded after 3 days and cured in lime saturated water at 20±3^{0}C until the time of testing.

The microstructure of the pastes was examined after 1, 7, 28, 56, 90, 180, and 365 days of curing using a Philip 515 scanning electron microscope (SEM) operating in a secondary

Table 1. Chemical and Physical Properties of Cements and Fly Ash

	Cement	Class F ash	Class C ash
Physical Tests			
Specific gravity	3.14	2.23	2.45
Fineness			
-passing 45μm, %	94.9	78.6	72.7
-specific surface, Blaine, m^2/kg	376	221	239
Compressive strength of 51 mm cube, MPa			
-3-day	31.5		
-7-day	34.5		
-28-day			
Pozzolanic Activity Index, %		84.5	87.7
Chemical Analyses, %			
Silicon dioxide (SiO_2)	19.20	53.64	46.20
Aluminum oxide (Al_2O_3)	5.79	27.42	15.60
Ferric oxide (Fe_2O_3)	2.03	7.74	7.70
Calcium oxide (CaO)	63.48	2.88	14.93
Magnesium oxide (MgO)	2.52	0.99	4.34
Sodium oxide (Na_2O)	0.33	0.38	5.52
Potassium oxide (K_2O)	1.16	2.42	1.86
Phosphorous oxide (P_2O_5)	0.10	0.34	0.18
Titanium oxide (TiO_2)	0.28	1.66	0.74
Mangnese oxide (MnO)	0.06	0.02	0.03
Sulphur trioxide (SO_3)	3.50	0.37	1.72
Loss on ignition	2.61	1.49	0.45
Total	101.06	99.35	99.27
Bogue Potential Compounds			
Tricalcium silicate C_3S	63.65		
Dicalcium silicate C_2S	7.03		
Tricalcium aluminate C_3A	11.91		
Tetracalcium alimonoferrite C_4AF	6.18		

Table 2. Mix Proportions of the Pastes

Nomenclature	Type of fly ash	Fly ash content (%)	W/C+F	SP content (% of C+F)
GB (E2)	Class F	58	0.3	1.2 (0.5)
GL (E3)	Class C	58	0.3	1.2 (0.5)

electron image (SEI) mode. The SEM was equipped with a Link exL energy dispersive X-ray analyzer. For the examination of the paste samples, fragments were taken from the center of each specimen such that all surfaces were free of the mold wall impression. Hydration was arrested by freeze-drying. The samples were coated with gold for the examination.

Selected paste samples were also examined by scanning electron microscope in a backscattered electron image (BEI) mode using polished sections. To prepare samples for BEI examination, a fragment of paste free of the mold wall were embedded and vacuum impregnated in a low viscosity epoxy resin*. The specimen was then polished using a series of diamond grits, finishing with 0.25 μm. Alcohol was used as a lubricant and coolant for cutting and polishing to avoid further cement hydration and dissolution of hydration products.

Samples for the examination of crack path were obtained by splitting cylinder specimens along the vertical diameter to introduce a crack path. A section of the sample containing a segment of the crack path was then embedded in epoxy and polished as described above.

All the polished specimens were coated with carbon and examined in a JEOL JSM 6400 scanning electron microscope.

The stress-strain relationship of the pastes under uniaxial compression was determined after 28, 56, 90, 180, and 365 days of curing. Three specimens for each mixture were tested using an MTS 815 system. Before testing, cylinders were cut to a length of about 120 mm by removing a portion from each end. The ends were then ground to make them parallel. The load was applied at a constant axial strain of 15 $\mu\varepsilon$/sec. Signals from the load cell and axial linear variable differential transformers (LVDTs) were scanned every 3 seconds and the data stored digitally.

RESULTS AND DISCUSSION

Microstructure

1. Paste with the Class F fly ash

Fig. 1 shows a micrograph of the paste cured for 1 day. Fly ash particles appear to be acting as sites for growth and deposition of C-S-H and sulphoaluminate (AF_t) hydrates produced through cement hydration with little evidence of significant reaction of the fly ash itself. By 7 days, circular deposits are noted in localized regions of some fly ash particles (Fig. 2). Etching of glassy materials is also visible on some ash particles (Fig.3).

By 28 days, many ash particles show etching of glassy material from the boundaries of crystals (probably mullite) oriented in the plane of the particle surface and in circular regions surrounding crystals oriented perpendicularly to the particle surface (Fig. 4). Also by 28 days, deposits of material, oriented radially to the fly ash surface, are observed as boundary zones around some ash particles (Fig. 5).

At various ages beyond 28 days, typical reaction products of round, toroidal plates, with

* Epofix resin (Struers)

Fig. 1. SEM micrograph of a part of a fly ash particle from the paste with Class F fly ash cured for 1 day. The fly ash particle appears to be covered partly by C-S-H and ettringite (AFt) hydrates.

Fig. 2. SEM micrograph of the paste with Class F fly ash cured for 7 days. Circular deposits are noted in localized regions of the fly ash particle on the left side of the picture.

Fig. 3. SEM micrograph of the paste with Class F fly ash cured for 7 days showing etching of glassy material on the ash particle in the center of the picture.

Fig. 4. SEM micrograph of a part of a fly ash particle from the paste with Class F fly ash cured for 28 days. It shows etching of glassy materials from the boundaries of crystals oriented in the plane of the particle surface and in circular regions surrounding crystals oriented perpendicularly to the particle surface.

compositions consistent with C-S-H, and a well defined hexagonal crystalline form were seen in the indentations formed by fly ash particles which were removed during fracturing (Fig.6). Because of the relatively small size of the hexagonal plates and the fact that most of them were embedded partly in the matrix of hydration products, it is difficult to determine their chemical composition by energy dispersive X-ray analysis.

Fig. 5. SEM micrograph of the paste with Class F fly ash cured for 28 days showing deposits of material, oriented radially to the surface of the fly ash particle in the center of the picture, as a boundary zone around the ash particle.

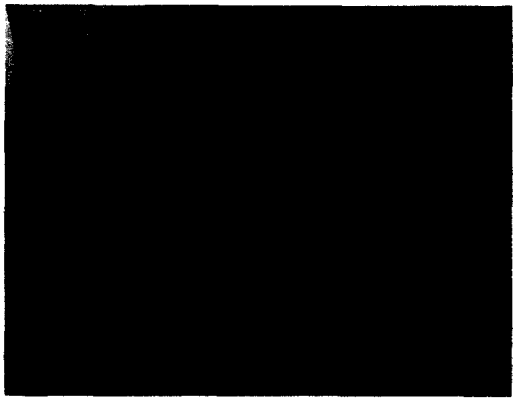

Fig. 6. SEM micrograph of an indentation formed by a fly ash particle removed during fracturing. The paste was made with Class F fly ash and cured for 56 days. Reaction products in the indentation comprise round, toroidal plates with compositions consistent with C-S-H and plates with a well-defined hexagonal crystalline form.

The electron microscopic examination reveals evidence for extensive ash reactions. However, it must be noted that even at 365 days, large proportions of the paste comprise spherical (though extensively etched) ash particles embedded in hydration products. These particles, though mostly etched, retain the spherical morphology typical of fly ash.

Figures 7 and 8 show backscattered electron images from the paste cured for 28 and 180 days,

Fig. 7. Backscattered electron image (BEI) of a polished section of the paste with the Class F fly ash cured for 28 days. There appears to be a porous zone around some fly ash particles, manifested as black rings around fly ash particles in the BEI.

Fig. 8. Backscattered electron image of a polished section of the paste with the Class F fly ash cured for 180 days. Significant densification has taken place at this age, although residual fly ash particles remain in the system.

respectively. At 28 days, there appears to be a porous zone around some fly ash particles, manifested as black rings around fly ash particles in the BEI. By 180 days, significant densification has taken place, although residual, typically spherical fly ash particles remain in large quantities in the system. Compared with the condition after 28 days, the microstructure of the paste is more unified and the hydration and reaction products are more evenly distributed in the system in general. The porous zone around the fly ash particles appears to have densified substantially, although some regions of higher porosity persist.

The observation of a porous zone between fly ash particles and the matrix of hydration and reaction products suggests that the bonding between these two phases may be weak at early ages of curing. Subsequent densification of these regions indicates that bonding may improve as curing continues. This improvement would increase the resistance to splitting stress, reduce the deformation under load, and increase the modulus of elasticity.

2. Paste with the Class C fly ash

For the paste containing the Class C fly ash, most of the fly ash particles were covered by a layer of fibrous CSH on the surface with ettringite filling porous spaces (Fig. 9) at 1 day. It is, therefore, difficult to determine whether there are reactions of the fly ash itself. Signs of fly ash reaction were visible at 7 days. A typical reaction product for this fly ash was a fibrous deposit oriented radially around the fly ash particles. X-ray analysis indicates that the deposit consists mainly of calcium and silicon, sometimes also aluminum. As the size of fly ash particles decreased with hydration and reaction, the radiating fibers probably grew inward to fill the space. It appears that the connection between the reaction products and the fly ash particles was relatively weak, thus many pits as shown in Fig. 10 were observed, where fly ash particles were probably pulled out from their original locations during the preparation of the sample. The observation is in agreement with that of Grutzeck et al. [6].

Fig. 9. SEM micrograph of the paste with the Class C fly ash cured for 1 day. Most of the fly ash particles were covered by a layer of fibrous CSH on the surface with ettringite filling porous space.

Fig. 10. SEM micrograph of the paste with the Class C fly ash cured for 7 days showing a pit where a fly ash particle was probably pulled out from its original location during the preparation of the sample.

Fig. 11. SEM micrograph of the paste with the Class C fly ash cured for 365 days. Some of the fly ash particles appear reacted completely, so the radially fibrous reaction product had grown inward filling the space originally occupied by the fly ash particle itself (e.g. "A" and "B").

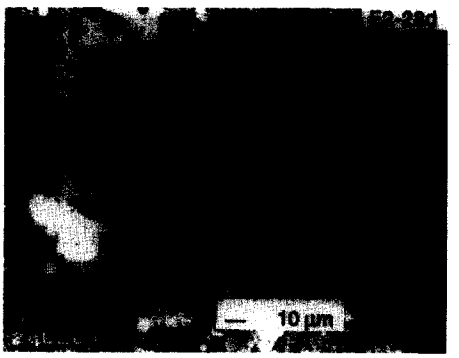

Fig. 12. Backscattered electron image of a polished section of the paste with the Class F fly ash cured for 28 days with the fracture path shown on the right side of the picture. Crack propagation deviated around fly ash particles.

Even by 365 days, there were still a large quantity of residual fly ash particles remained in the system. However, some of the fly ash particles appear reacted completely. The radially fibrous reaction product thus had grown inward filling the space originally occupied by the fly ash particle itself (Fig. 11).

It seems that the distribution of hydration and reaction products was relatively uneven in the system with this fly ash. Some areas appear very dense, while others relatively porous. Even by 365 days, ettringite could still be observed filling some porous space. This indicates a low mobility of the reaction products and may be attributed to a quick early hydration and reaction of the fly ash, which may hinder subsequent hydration and reactions as well as distribution of the hydration and reaction products.

The backscattered electron images of the paste with the Class C fly ash also show the relatively porous zone between the fly ash particles and the matrix of the hydration and reaction products as that observed in the paste with the Class F fly ash.

Crack Pattern

Baldie and Pratt [7] examined Portland cement paste with introduced cracks. They found that for portland cement pastes, crack propagation passes almost exclusively through calcium silicate hydrate and $Ca(OH)_2$, making significant deviation around unhydrated cement particles. They also observed that the rims of inner calcium silicate around C_3S appear to be strongly bonded to the underlying C_3S, whereas not well bonded to C_2S and interstitial material. They suggested, therefore, that the unhydrated cement cores may act as "microaggregate" in cement paste. However, microcracking was not observed at the immediate core/hydrate bond. In concrete, the aggregate/mortar matrix is believed to be the nucleation site for microcracks which coalesce to form a macro-crack as fracturing progresses.

The fracture of the fly ash pastes has some features in common with Portland cement pastes, but also has their own characteristics. Crack propagation generally deviated around fly ash particles (Fig. 12). In some circumstances, the surface layers (outer regions) of the fly ash particles were fractured as well. This may simply be because of a higher porosity in the outer region of certain fly ash particles as a result of hydration and reactions. By 365 days, crack paths were straighter than those at early ages due to, at least partly, a reduced size of the fly ashes, though cracks still deviated around fly ash particles.

In the HVFA pastes, fly ash particles are generally much harder, stronger, and of a higher modulus of elasticity than the matrix of hydration and reaction products because of their glassy nature. The difference of the modulus of elasticity between two phases in a material generally causes stress concentration when the material is subjected to various loadings.

As an example, Fig. 13 shows a general model of stress distributions in concretes as two-phase composites with a coarse aggregate particle embedded in a continuous mortar matrix when they are subjected to compressive loading. The stress distribution is determined primarily by the relative modulus of elasticity between the two phases. Under the condition where the interfacial zone between the aggregate and the matrix is weaker than either the aggregate or the matrix, if the modulus of elasticity of the aggregate is higher than that of the matrix, tensile stress will develop in the interfacial zone. If the tensile stress exceeds the tensile strength, cracks will deviate around the aggregate (Fig. 13(a)). If the modulus of elasticity of the aggregate is lower than that of the matrix and the interfacial zone, tensile stress will develop immediately above and below the aggregate and, therefore, cracks will often go through the aggregate (Fig. 13(b)). The magnitude of this tensile stress is influenced not only by the elastic modulus of both phases but by the size of the aggregate as well.

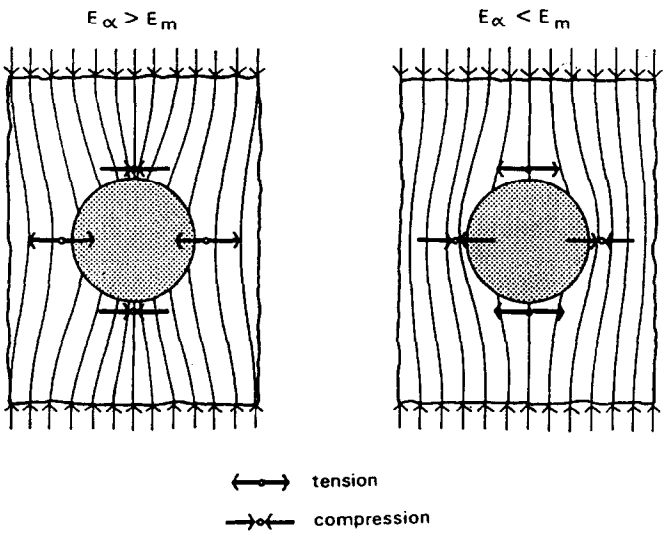

Fig. 13. General model of the stress distribution when two-phase composites with a spherical inclusion embedded in a matrix are subjected to compressive loadings. $E\alpha$=modulus of elasticity of inclusion; E_m=modulus of elasticity of matrix [8].

The fracture pattern observed in the fly ash pastes is consistent with a weak bond between fly ash particles and the matrix of hydration products discussed in the previous section. Alternatively, the same type of fracture might result from the fly ash particles having a higher modulus of elasticity than the matrix of hydration products. Such differences in modulus of elasticity would cause stress concentrations in the bond area discussed above. For the high volume fly ash pastes, it is probable that both weak bonding and stress concentration effects operate simultaneously. In either case the fly ash particles appear to function as microaggegates in the paste. Thus, the HVFA paste may be considered as a composite material microscopically.

Stress-strain relationship

The shape of the stress-strain relationship is generally related to physical characteristics as well as internal microcracking of materials. Because of such a relationship, a stress-strain curve may be used as a means to determine indirectly the homogeneity of the material and some characteristics of the fracture.

Figure 14 shows typical stress-strain curves for concrete, its aggregate component, and its cement paste component with a compressive strength of about 35 MPa as an example. The stress-strain curve of the aggregate shows linearity to failure, consistent with its generally homogeneous nature. The stress-strain curve of the cement paste is similarly linear to about 90% of its strength, indicating good homogeneity. The stress-strain curve of the concrete, being inhomogeneous, deviates greatly from linearity at the stress less than 50% of the strength. This deviation from the linearty has been related to the bond cracks between coarse aggregate and mortar matrix [10].

The stress-strain curves (Figs. 15 and 16) for the two HVFA pastes examined indicate that both pastes behave as non-homogeneous materials.

Compared with that of the Portland cement paste of similar strength (see Fig. 14), the stress--strain curves for the paste with the Class F fly ash (Fig. 15) and the paste with the Class C fly

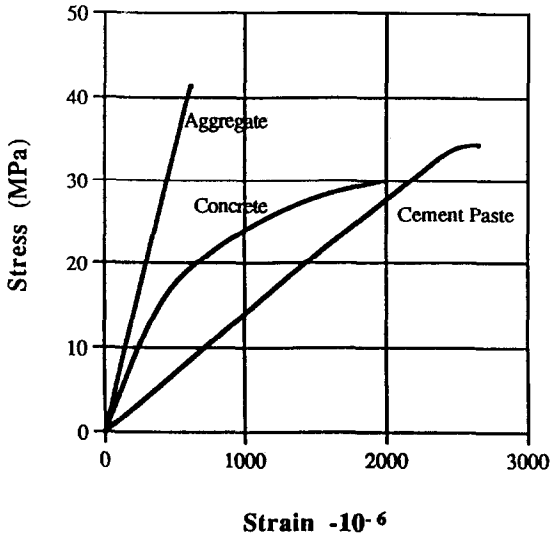

Fig. 14. Stress-strain relations for cement paste, aggregate, and concrete [9].

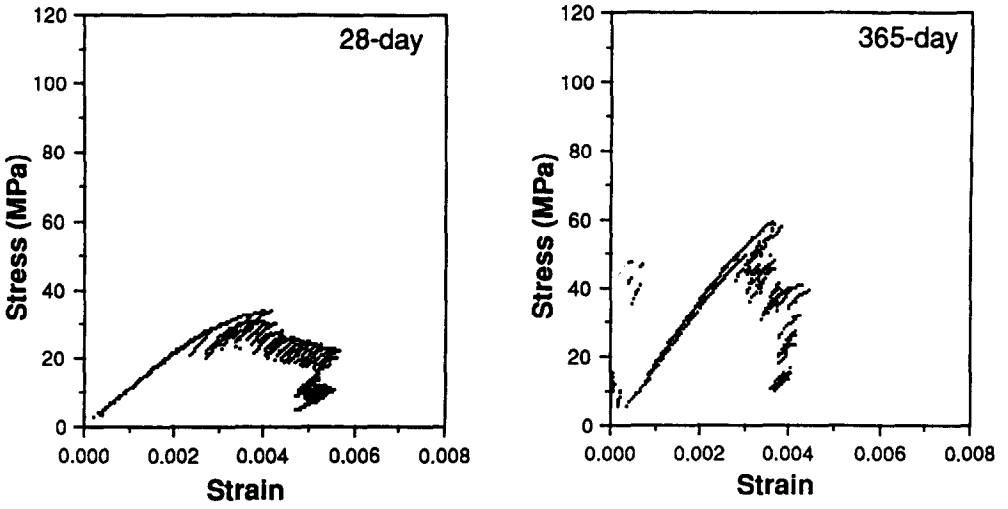

Fig. 15. Stress-strain curves for the paste with the Class F fly ash at 28 and 365 days.

ash (Fig. 16) are less linear and begin to deviate at about 65-70 % and 60-65 % of the ultimate strengths at 28 days, respectively. This is probably related to the increase of cracks between the fly ash particles and the hydrates with the increase of loading. With further curing, the stress-strain curves become steeper, and deviate from linearity at higher stress/strength ratios (~85% of ultimate strength at 365 days for both pastes) indicating an improvement of bond and densification of the matrix. The densification of the matrix of hydration and reaction product as well as the leaching of substances from the fly ash particles with time may reduce the difference in the modulus of elasticity, and consequently reduce the stress concentration between the fly ash particles and the matrix of hydration and reaction products. The reduction of such a stress concentration, together with the improvement of bonding between the fly ash particles and the matrix explains the higher stress levels at which stress-strain curves deviate from the linearity for the HVFA pastes at later ages.

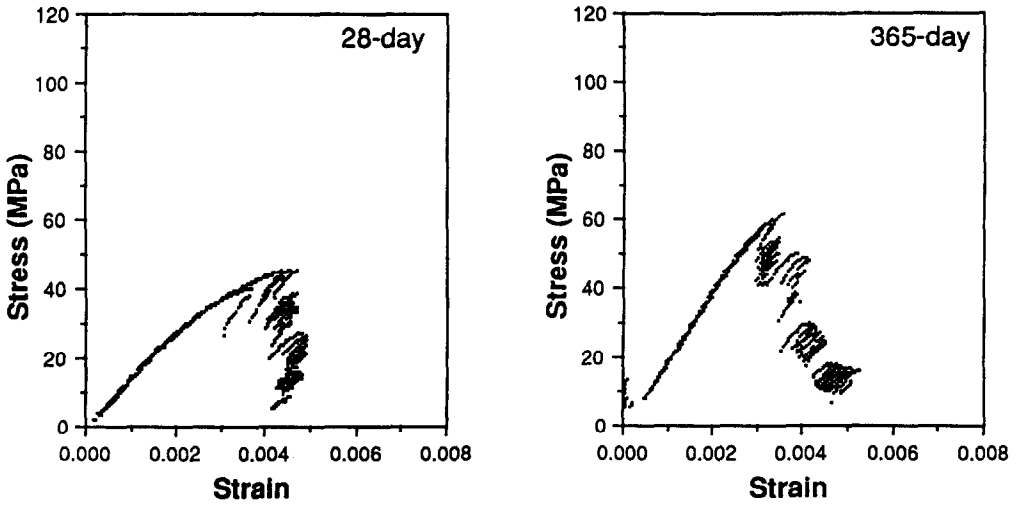

Fig. 16. Stress-strain curves for the paste with the Class C fly ash at 28 and 365 days.

Proposed model of HVFA paste as a composite

A composite material is defined as a solid which is made by physically combining two or more existing materials to produce a multi-phase system with different physical properties from the starting materials. Some chemical interactions often occur in the process, so that one phase may differ from the starting materials, but in many cases the phases remain substantially unchanged. In addition, an interface may be formed at the phase boundaries, which may differ from the starting materials.

The microstructure and the crack pattern, together with the evidence of the deviation of the stress-strain curves from linearity indicate that the HVFA pastes may be considered as composite materials microscopically. Fly ash particles in the HVFA pastes may act in part as reactive microaggregates embedded in a matrix of hydration and reaction products. In addition, there is an interfacial zone between the fly ash particles and the matrix, which is more porous and weaker than either the fly ash particles or the matrix of hydration and reaction products.

The proposed model may be used to explain some observed properties of HVFA concretes, for example, the higher modulus of elasticity, lower shrinkage and creep, as well as lower water permeability [4].

The modulus of elasticity of a composite is dependent on the modulus of elasticity of each component, the bond between them, and the relative volume of each component. The improvement of the bond between the fly ash particles and the matrix makes the fly ash particles become a more effective part of the material. Therefore, the HVFA paste would have a high modulus of elasticity due to the contribution of high modulus of elasticity of the fly ash particles. As concrete can be considered as a composite material with coarse aggregate bonded together by mortar; mortar with sand particles bonded by cement paste; Portland cement paste with unhydrated cement particles embedded in the matrix of hydration products; or HVFA paste with fly ash particles embedded in the matrix of hydration and reaction products, the higher modulus of elasticity of the HVFA concrete compared with portland cement concrete of similar strength observed by Carette et al. [2] may be attributed to the high modulus of elasticity of HVFA paste.

Another effect of fly ash particles as microaggregates with a higher modulus of elasticity than that of the matrix of hydration and reaction products is the restriction of deformations such as drying shrinkage and creep of the HVFA pastes. Consequently, the shrinkage and creep of the HVFA concrete may be reduced. Data on the drying shrinkage and creep reported by CANMET [2] supported this concept.

According to reference [4], the HVFA concretes showed a very low water permeability. For the HVFA concretes, in addition to the pozzolanic reaction normally considered to contribute to the low water permeability, there may be several other factors affecting the resistance of concrete against water intrusion. As discussed before, fly ash particles have a glassy nature and are generally much denser than surrounding hydration and reaction products. Even though the density and the size of the fly ash particles were reduced with continuous curing, the density of the remaining fly ash particles may still be higher than that of the matrix of hydration and reaction products. With the continuous hydration and reactions of the HVFA pastes and the improvement of the bond between the fly ash particles and the matrix, the fly ash particles become more effective inclusions in the system. This may contribute positively to the

resistance of the HVFA concretes against water intrusion. Also since a part of the paste volume may be occupied by fly ash particles even after a long term curing, the hydration and reaction products are required to fill a much smaller space compared with that of Portland cement paste of similar strength. This may be another factor contributing to the good resistance of the HVFA concrete against water intrusion. It is unclear at this stage, however, whether the interfacial zone between coarse aggregates and mortar matrix is improved by the incorporation of high volume of fly ash in the concrete, which is an important factor affecting the resistance of the concrete against water intrusion.

Overall, the HVFA pastes behave as composite materials that are subjected to changes in terms of the nature, quantity, and properties of the various phases as curing progresses.

SUMMARY AND CONCLUSIONS

Based on the limited number of experiments conducted, the following conclusions can be drawn:

(1) For the HVFA paste with the Class F fly ash, indications of leaching and reaction of the fly ash were observed initially at 7 days, however, even after 365 days of hydration and reaction, there still exist residual fly ash particles and calcium hydroxide in the pastes. Typical reaction products around the fly ash were round, toroidal plates with compositions similar to C-S-H and hexagonal plates.

(2) For the fly ash paste with Class C fly ash, signs of fly ash reaction were also visible at 7 days. A typical reaction product around this fly ash was a radially fibrous material. The chemical composition of the material consists mainly of calcium and silicon, sometimes also aluminum.

(3) A region develops around the fly ash particles which appears to be the reaction products of fly ash. This zone of reaction products appears porous under the SEM, which indicates that the bond between the fly ash particles and the matrix of hydration and reaction products is relatively weak. The level of porosity, however, appears to be substantially reduced at later ages.

(4) For the pastes with the fly ashes, crack propagation generally deviates around the fly ash particles. This is consistent with the bond between fly ash particles and the matrix of hydrates being weak and/or the higher modulus of elasticity of the fly ash particles compared to the matrix of hydrates.

(5) Compared with that for the Portland cement paste of similar strength, the stress-strain curves for the HVFA pastes are less linear and begin to deviate at about 60-70% of the ultimate strength at 28 days.

(6) Fly ash particles in HVFA pastes appear to act in part as reactive microaggregates. Overall, the HVFA pastes behave as composites microscopically that are subject to changes in terms of the nature, quantity and properties of the various phases as curing progresses.

ACKNOWLEDGEMENT

The work was carried out while the author was a research engineer at Radian Canada Inc. The author would like to thank the Electric Power Research Institute for financial support of this investigation under EPRI contract RP3176-06. Particular thanks are due to Dr. Edwin Berry, Dr. Ray Hemmings of Radian Canada Inc., and Mr. Dean Golden of EPRI for valuable discussion. Thanks are also due to Mr. H. Dean Dodgen of the Georgia Power Co. and Mr. William E. Gross of Basin Electric Power Co. for providing fly ashes for use in this project.

REFERENCES

1. Malhotra, V.M. "Superplasticized Fly Ash Concrete for Structural Concrete Applications," *Concrete International,* Dec. 1986, pp. 28-3 1.
2. Carette, G.G., Bilodeau, A., Chevrier, R., and Malhotra, V.M., "Mechanical Properties of Concrete Incorporating High Volumes of Fly Ash from Sources in the U.S.A.," Supplemental Proceedings: Fourth CANMET/ACI Int. Conf. on Fly Ash, Silica Fume, Slag and Natural Pozzolans in Concrete, High-Volume Fly Ash Concrete Session, Istanbul, Turkey, May 1992.
3. Bilodeau, A., Sivasundaram, V., Painter, K.E., and Malhotra, V.M., "Durability of Concrete incorporating High Volumes of Fly Ash from Sources in the U.S.A.," Supplemental Proceedings: Fourth CANMET/ACI Int. Conf. on Fly Ash, Silica Fume, Slag and Natural Pozzolans in Concrete, High-Volume Fly Ash Concrete Session, Istanbul, Turkey, May 1992.
4. "Investigation of High-Volume Fly Ash Concrete System," EPRI report TR-103151, Oct. 1993.
5. Berry et al., "Hydration in High Volume Fly Ash Binders: Chamical Factors," *ACI Materials Journal*, Vol.91, No. 4, July-August 1994, pp. 382-389.
6. Grutzeck, M.W., Roy, D.M., and Scheetz, B.E., "Hydration Mechanisms of High-Lime Fly Ash in Portland-Cement Composites," Proc. of Materials Research Society Symposium N, Effect of Fly Ash incorporation in Cement and Concrete, Boston, Massachusetts, Nov. 1618, 1981, pp. 92-101.
7. Baldie, K.D. and Pratt, P.L., "Crack Growth in Hardened Cement Paste," Materials Research Society Symposia Proceedings Vol. 64, "Cement Based Composites: Strain Rate Effects on Fracture," Boston, Massachusetts, Dec. 4-5, 1985, pp. 47-61.
8. "FIP Manual of Lightweight Aggregate Concrete, 2nd Ed.," published by Surrey University Press, Glasgow and London, and Halsted Press, a Division of John Wiley and Sons, New York - Toronto, 1983.
9. Neville, A.M., "Properties of Concrete, 3rd Ed," Longman Scientific & Technical, copublished by John Wiley & Sons, 1981, pp. 364.
10. Shah, S. P. and Slate, F. O., "Internal Microcracking, Mortar-Aggregate Bond and the Stress-Strain curve of Concrete," Proc. of the International Conference on the Structure of Concrete, Paper B3, London, Sept. 1965.